Impregnation and encapsulation of lightweight aggregates for self-healing concrete

R. Alghamri *, A. Kanellopoulos, A. Al-Tabbaa

Department of Engineering, University of Cambridge, Cambridge CB2 1PZ, UK

HIGHLIGHTS

- Sodium silicate solution was impregnated in lightweight aggregates (LWA).
- Impregnated LWA were coated then embedded in concrete specimens.
- Strength regain was remarkable for specimens with the impregnated LWA.
- Capillary water absorption was significantly improved in the specimens with the impregnated LWA.
- Sodium silicate produced rich silica C–S–H to heal the concrete cracks.

ARTICLE INFO

ABSTRACT

This study investigated a technique of impregnating potential self-healing agents into lightweight aggregates (LWA) and the self-healing performance of concrete mixed with the impregnated LWA. Lightweight aggregates with a diameter range of 4–8 mm were impregnated with a sodium silicate solution as a potential self-healing agent. Concrete specimens containing the impregnated LWA and control specimens were pre-cracked up to 300 μm crack width at 7 days. Flexural strength recovery and reduction in water sorptivity were examined. After 28 days healing in water, the specimens containing the impregnated LWA showed ~80% recovery of the pre-cracking strength, which accounts more than five times of the control specimens' recovery. The capillary water absorption was also significantly improved; the specimens healed with the impregnated LWA showed a 50% reduction in the sorptivity index compared with the control cracked specimens and a very similar response to the control uncracked specimens. The contribution of sodium silicate in producing more calcium silicate hydrate gel was confirmed by characterisation the healing products using X-ray diffraction, Fourier transform spectroscopy, and scanning electron microscopy.

1. Introduction

Surface opening cracks are a common type of defects in concrete structures. They allow penetration of water or other deleterious agents that result in loss of durability earlier than expected. Thus, repairing formed cracks and defects becomes essential and unavoidable. Currently, maintenance and repair of concrete structures generally rely on regular inspection programmes, which are expensive, and they also depend on a combination of non-destructive testing (NDT) and human perception [1]. In case of severe damage, the structural component is replaced entirely while repairs are attempted for less extensive damage. Vast amounts of money are spent each year on inspection and repair as direct and indirect costs, the latter often being much higher than the former. For instance, in the USA, the annual economic impact associated with maintaining, repairing, or replacing deteriorating structures is estimated at $18–21 billion [2]. The American Society of Civil Engineers estimated that $2.2 trillion are needed for five years, starting from 2012, for repair and retrofit; a cost of $2 trillion has been predicted for Asia's infrastructure for the same period [3]. Europe spends more than half of its annual construction budget on repair works [4], while in the UK, repair and maintenance costs account for over 45% of the total expenditure on construction [5].

Moreover, repair works have a significant adverse environmental impact particularly in cases where partial or complete replacement of structures is required. It is known that the production of 1 tonne of Portland cement (PC), as often being the main constituent

---

* Corresponding author.
  E-mail addresses: rja75@cam.ac.uk (R. Alghamri), ak880@cam.ac.uk (A. Kanellopoulos), aa22@cam.ac.uk (A. Al-Tabbaa).

on concrete, releases about 0.85–1.1 tonnes of CO_2 [6]. Approximately 3.6×10^9 tonnes of cement were produced worldwide in 2014 [7]. The CO_2 emissions associated with the production of cement are very significant, and are estimated at 7% of the global anthropogenic CO_2 emissions [6].

Therefore, developing innovative technologies to overcome these challenges has become an urgent necessity. Over the past few decades, the notion that concrete can be designed with a sufficient healing capability and heal its cracks without any external aid has been inspiring field of work for many research groups around the world. Self-healing as defined by RILEM is "any process by the material itself involving the recovery and hence improvement of a performance after an earlier action that had reduced the performance of the material" [8].

Broadly, self-healing processes within cement based materials can be divided into two categories: autogenic and autonomic. Autogenic self-healing is the phenomenon where the material heals cracks using its own generic components and constituents. Autonomic self-healing however, involves the use of engineered additions that are not conventionally added into cementitious materials. These additions are added specifically to enhance self-healing capability[8,9].

The main mechanisms of the autogenic self-healing are the ongoing hydration of cement grains that have not reacted due to lack of water or the precipitation of the calcium carbonate, which is the result of a reaction between the calcium ions in concrete and carbon dioxide dissolved in water [8,10]. Ongoing hydration is the main healing mechanism in young concrete due to its relatively high content of un-hydrated cement particles, while formation of calcium carbonate is the most likely cause of self-healing at later ages [11]. For attaining effective autogenous self-healing, water is essential and the crack widths are restricted to be less than 100 μm and preferably less than 50 μm [12,13]. Some studies have been carried out to promote autogenous healing by crack width restriction or with continuous supply of water. For instance, fibre reinforced cementitious composites (FRCC) have significantly higher potential of self-healing than ordinary concrete because of their high ductility, the micro-cracking behaviour and tight crack width control [11,14]. Several fibres have been used in FRCC composites such as polyethylene (PE) [15], polyvinyl alcohol (PVA) [16–18], and polypropylene (PP) fibres [18]. Meanwhile some researchers have investigated the possibility to mix super absorbent polymers (SAP) into cementitious materials to provide additional water [19,20]. Others have examined the effect of replacing part of the cement by other pozzolanic and latent hydraulic materials like fly ash, silica fume, or blast furnace slag [21–24]. These materials continue to hydrate for prolonged time enhancing the autogenous healing potential.

In contrast, many systems and techniques have been investigated to heal concrete cracks autonomically such as modifying concrete by embedding microcapsules or hollow fibres with a suitable healing agent. Once the crack occurs the shell of the capsule or the wall of the tube ruptures and the healing agent is released and reacts in the region of damage to produce new compounds which seal the crack and/or bond the crack faces [3]. Zhao et al. [25] have reported that the most utilised shell polymers in development the microcapsules are poly(urea-formaldehyde) (PUF), polyurethane (PU) and poly(melamine-formaldehyde).The healing agents that have been often used to date in the literature include epoxy resins [26,27], methyl methacrylate (MMA) [28], alkali-silica solutions (Na_2SiO_3) [29], and cyanoacrylates (CA) [30–32]. Additionally, bacterially induced carbonate precipitation has been proposed as an alternative and environmental friendly self-healing technique [33–35]. Other researchers proposed the use of expansive agents and swelling geo-materials to stimulate the chemical reactions to produce hydration products for filling cracks in concrete [14]. For

instance, Kishi and co-workers (2007) have demonstrated the use of a mix of expansive agents (C_4A_3S, $CaSO_4$, and CaO), swelling geo-materials such as silicon dioxide and sodium aluminium silicate hydroxide, montmorillonite clay and various types of carbonates as partial cement replacement [36]. Ferrara et al. [37] and Roig-Flores et al. [38] have investigated the self-healing behaviour of ordinary concrete mixtures included crystalline admixture additives, which consist of a mix of cement, sand and active silica. Calcium sulfoaluminate (CSA) has also been utilised as an expansive agent for self-sealing [36,39,40] and recently magnesium oxide has been suggested as a self-healing agent by Alghamri and Al-Tabbaa [41].

Sodium silicate (Na_2SiO_3) has been proposed as a potential self-healing agent in different systems. A number of researchers have assessed different aspects of the self-healing capability of sodium silicate. Pelletier et al. [42] enveloped crystalline sodium silicate in polyurethane microcapsules with 40–800 μm size. Thereafter, the synthesised capsules were added to concrete mix of 2% by volume. The concrete samples containing the microcapsules showed 24% flexural strength recovery compared with 12% for the control samples. Huang and Ye [29] embedded 5 mm diameter capsules filled with sodium silicate solution into specimens of engineering cementitious composites (ECC). The results demonstrated that the main mechanisms of self-healing are the reaction between the calcium cations and the dissolved sodium silicate and the crystallisation of the sodium silicate. However, the results showed also a negative effect of the capsules on the mechanical properties of concrete specimens. In another study, Gilford et al. [43] developed sodium silicate and dicyclopentadiene (DCPD) as self-healing agents encapsulated in urea-formaldehyde shell. The two types of microcapsules were examined in concrete cylinder specimens. The results indicated that the addition of 5% sodium silicate microcapsules by weight of cement increased the modulus of elasticity of the concrete specimens by 11% after healing. For the DCPD microcapsules, the healing agent was effective in increasing the modulus of elasticity of concrete after cracking by as much as 30% for the microcapsules at a content of 0.25%. Mostavi et al., [44] also used double-walled polyurethane/urea-formaldehyde (PU/UF) microcapsules to encapsulate sodium silicate. These microcapsules were incorporated into concrete beams with two different proportions (2.5% and 5% by weight of cement) and the healing process was monitored by measuring the crack depth within the healing time using ultrasonic digital indicating tester. It was found that the healing rate with 5% microcapsules was higher in comparison with samples containing 2.5% of microcapsules. In a recent study conducted by Kanellopoulos et al. [45], liquid sodium silicate was stored in a thin walled soda glass capsules. The results indicated that the sodium silicate has a promising capability as a self-healing agents in both regaining strength and improving durability.

Given that the aggregates are the major constituent of any concrete mix, they had been expected to be widely used to host self-healing agents: however, this potential has not been extensively researched. In a study performed by Wiktor and Jonkers [34], porous clay particles with (1–4) mm size were impregnated twice under vacuum by a two-component bio-chemical self-healing agent consisting of bacterial spores and calcium lactate. Upon crack formation the two components were released from the particles by crack ingress water and produced calcium carbonate which led to plug cracks of up to 0.46 mm width. In another study, Sisomphon et al. [46] used expanded clay lightweight aggregates as reservoirs for sodium monofluorophosphate (Na_2FPO_3) solution and eventually encapsulated them in a cement paste layer. The developed encapsulated particles were used as a self-healing system in blast furnace slag cement mortars. The characterisation of the healing products indicated that the healing mechanism would

be due to the combination of treatment by Na_2FPO_3 solution and calcium hydroxide supplied from the cement paste coating layer. However, these studies presented limited data regarding the impregnation technique and the influence of replacing the aggregates partially or completely by the impregnated ones on the mechanical properties.

Thus, this paper aims at studying the vacuum impregnation technique as a system for hosting a self-healing agent into lightweight aggregates (LWA). Sodium silicate was selected as a potential self-healing agent by impregnating it into (4–8) mm LWA particles, which then were encapsulated in a polymer based coating.

2. Materials and methods

2.1. Materials

The main materials used in the preparation of impregnated lightweight aggregates and concrete mixes are as follows:

(a) *Sodium silicate:* Sodium silicate solution obtained from Sigma-Aldrich, UK, with the properties shown in Table 1 was used as the self-healing agent in this study.
(b) *Aggregates:* Coarse and fine lightweight aggregates (LWA) supplied by Lytag Ltd, UK, were used in this study. Only the coarse LWA were utilised for impregnation. The properties of both fine and coarse Lytag are summarised in Table 2.
(c) *Cement:* The cement used in this study was CEM I (52.5 N) with a particle density of (2.7–3.2) g/cm³ and a specific surface area of (0.30–0.40) m²/g, which was supplied by Hanson, UK. The chemical composition of the cement is shown in Table 3.

2.2. Impregnation and coating procedure

The coarse LWA with 4–8 mm diameter were dried in the oven at a temperature of 60 °C for 3 days followed by 24 h in the vacuum desiccator. Preliminary studies were performed to test the absorption rate of the dried aggregates under immersion and impregnation processes. In case of immersion, the aggregates were just immersed in a sodium silicate solution in a climate controlled room under conditions of 20 ± 2 °C and $50 \pm 5\%$ RH: they were immersed for different periods (1, 2 and 3 days). Their weight was monitored at the end of each period using a digital scale with 0.1 g accuracy. A set-up for the impregnation process shown in Fig. 1 was developed in laboratory. It consists of an acrylic vacuum chamber with three ports (vacuum, vent, and gauge) and connected with an appropriate vacuum pump. The aggregates were loaded into the vacuum chamber, which was then closed tightly and pressurised up to −0.7 bar for an hour. Thereafter, the sodium silicate solution was allowed into the chamber. The level of the sodium silicate into the chamber was raised to 20 mm above the aggregates level to ensure that all aggregates were immersed.

Fig. 2 shows the absorption rates for the two different methods. Preliminary results indicated that the absorption rate of immersed LWA reached up to 19% by weight after 3 days soaking in sodium
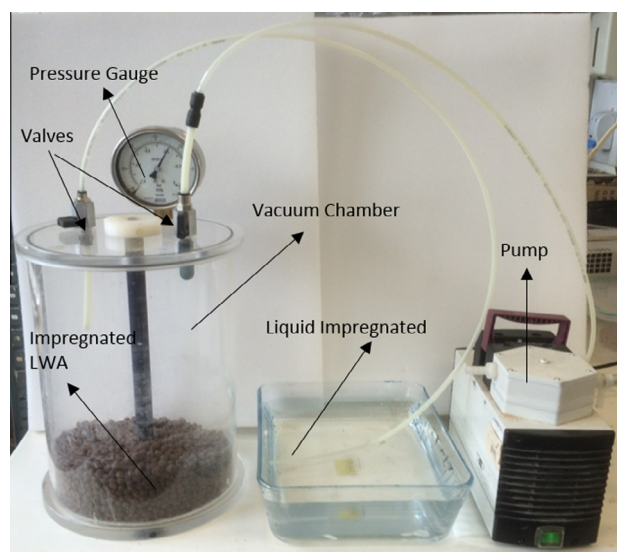
Table 1
The chemical and physical characteristics of the sodium silicate used.

Materials	Properties				
	Formula	Mw (gmol⁻¹)	Density @ 20 °C (g/mL)	Viscosity (cps) @ 20 °C	pH
Sodium silicate	Na_2O $(SiO_2)_x \cdot xH_2O$	122.06	1.39	60	12.5

Table 2
Properties of coarse and fine LWA used in this study as provided by the manufacturer.

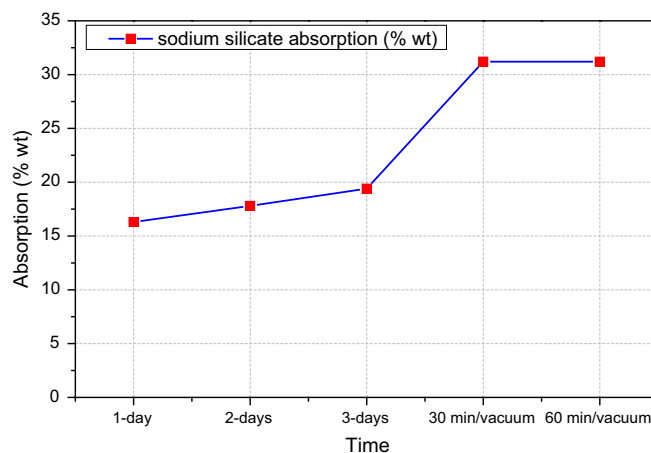| Properties (unit)	Coarse LWA	Fine LWA
Size (mm)	4–8	0–4
Declared oven dry loose bulk density (kg/m³)	710 ± 100	900 ± 100
Particle density (kg/m³)	1310	1350 ± 150
Material shape	Rounded	Angular
Typical moisture content as delivered (%)	15	15
Long term maximum moisture content (%)	30	30
Aggregate crushing Strength (N/mm²)	7	–

Table 3
Chemical composition of cement as provided by the manufacturer.

Materials	Composition (%)						
	CaO	SiO₂	Al₂O₃	Fe₂O₃	MgO	SO₃	LOI
Cement	63.60	19.50	4.90	3.10	0.90	3.30	2.10

Fig. 1. Vacuum impregnation set-up.

Fig. 2. Sodium silicate absorption of the lightweight aggregates.

silicate. When vacuum impregnation was used for 30 min the absorption percentage was raised to as high as 31%. This could be due to the effect of vacuum mechanism as it evacuates air from the voids which subsequently filled with the impregnated

Fig. 3. Coating the impregnated LWA.

material. Thus, it can be concluded here that the absorption rate was increased significantly by using vacuum compared with immersion under atmospheric condition. Increasing the vacuum impregnation time to 60 min did not increase further the absorption levels.

At the end of the 30 min' vacuum impregnation the excess sodium silicate solution was filtered and the aggregates' surface was dried with tissues. This resulted in saturated but surface dry particles. In order to prevent any potential leakage of the sodium silicate out of the aggregates or any premature interaction with the cementitious matrix the impregnated aggregates were coated with a polyvinyl alcohol (PVA) based coating using the spray coating method. PVA was obtained from Fisher Scientific as a 98–98.8% hydrolysed powder and an average molecular weight of 146,000–186,000. The spray gun used in the coating process is Gravity Feed Mini-HVLP gun with 1 mm nozzle size. During rotation of a disc pelletiser as shown in Fig. 3, the aggregates were sprayed with the coating solution with simultaneous drying by blowing a stream of hot air. Thereafter, the encapsulated LWA impregnated with sodium silicate (here referred to as EI-LWA), were stored in an airtight plastic container until used in the concrete mixes.

2.3. Concrete samples and curing

Targeting 30 N/mm^2 compressive strength, two mixes of lightweight concrete as indicated in Table 4 were prepared according to the technical manual of mix designs for Lytag concrete [47].

The first mix was the control and referred as (CN). In the second mix the coarse aggregates were replaced by the same volume of EI-LWA particles and this mix is referred to as (SHM). For both mixes, prism specimens with dimensions of 50 mm × 50 mm × 220 mm were prepared. A 1.6 mm diameter steel wire was placed at the top half of the specimen with a cover of 10 mm to prevent the specimen from breaking completely into two pieces when inducing the crack. All specimens were demoulded after 1 day of curing and

Table 4
Composition of concrete mix per m^3.

Ingredient	kg/m^3
Cement	360
Water	180
Fine LWA 0/4	405
Coarse LWA 4/8	525

then cured in a water tank at a room temperature of 20 ± 2 °C until the designed testing age. The experimental program to investigate the self-healing performance of both CN and SHM mixes is illustrated in Table 5.

The mechanical loading of the prisms was conducted by using a 30 kN INSTRON static testing frame. A three-point bending test controlled by the crack mouth opening displacement (CMOD) at the mid-span was performed for all specimens. Prior to cracking, a 1.5 mm deep notch, which serves as a crack initiating point was sawn on the underneath of each specimen at the mid-point. Prior to the testing, a CMOD clip gauge was mounted at the bottom face of the samples to measure the CMOD as shown in the experimental set-up (Fig. 4). A crack with a controlled width of 0.30 mm was induced in each prism at age of 7 days. In compliance with BS EN 12390-5:2009, the testing prism was placed upon a base of two supports with a span of 150 mm. Then the loading shaft was settled at the mid span and gently moved into contact with the prism top surface. The ramp speed was adjusted into 0.1 mm/min. After cracking, all samples were returned in the curing water tank. The cracked samples were placed vertically into the water tank in order to keep the crack surface in contact. The nine cracked specimens were divided into two groups: six of them were used for strength recovery tests and then characterisation of the healing products; the other three were used for sorptivity testing.

2.4. Evaluation of cracks sealing by optical microscopy and ultrasonic measurements

Digital microscope image analysis was used to analyse the sealing of crack surfaces in various periods as stated in Table 5. GXCAM 1.3 type digital microscope supplied by GT Vision Ltd was used. Specimens were removed from water weekly for stereomicroscopic inspection and photographic imaging for quantification of crack-healing in time. Cracked prisms were marked in different places and their widths were measured after initial cracking. It is noteworthy that despite the specimens were cracked for a controlled width of 0.30 mm, upon load removal all specimens had remaining crack width of 0.12–0.17 mm.

Furthermore, monitoring of the crack depth was carried out using the ultrasonic pulse velocity method. The ultrasonic equipment used is the PUNDIT-PL 200. The crack depth for all specimens was measured for different ages according to the experimental program shown in Table 5. As shown in Fig. 5(a), two 150 kHz transducers were used to measure transmission time t1 and t2 of the pulse to transit for distances 2b and 4b respectively as illustrated schematically in Fig. 5(b). Accordingly, the device calculates the depth of crack based on the transmission path of ultrasonic waves. The cracks affect the propagation of waves through the concrete specimens. Since ultrasonic waves travel much faster in hardened concrete (4000 m/s–5000 m/s) than in water (1480 m/s) or in air (350 m/s), they will travel around an open fissure leading to an increase in transmission time. However, when the crack is sealed, the waves will be able to travel through the sealant or the healing products and this reduces the travel time [33,37]. For each specimen, the test was repeated three times and the mean reading was adopted.

2.5. Flexural strength recovery

To examine the strength recovery, six specimens from each mix were re-cracked for the second round until failure at 28 days after the first crack. Three of them were returned back to the water tank for testing any further potential healing of the new cracks. After further 28 days, they were cracked for the third round until failure as well. According to BS EN 12390-5:2009, the flexural stress and strain were calculated using Eqs. (1) and (2).
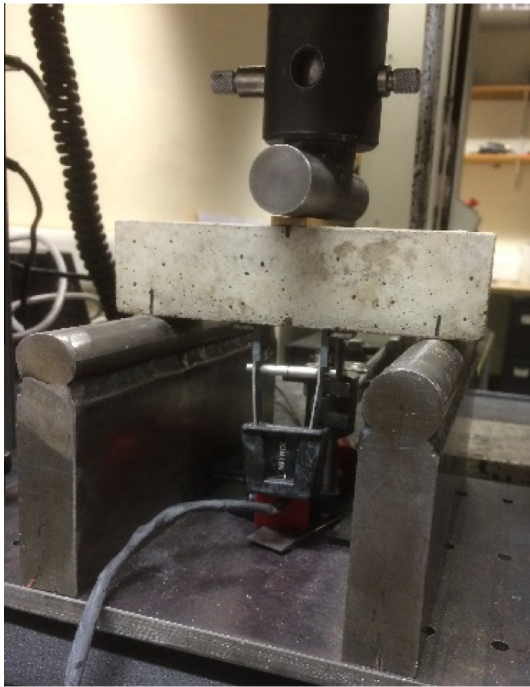
Table 5
Experimental program for investigating the self-healing performance of concrete samples.

Mix and cast	No. of specimens	Time (days)			
		1	7	7 + 28	7 + 28 + 28
• Preparation of two concrete mixes (CN and SHM). • Casting of 12 specimens for CN mix and 9 specimens for SHM mix. • Dimensions of the specimens are (50 mm × 50 mm × 220 mm).	3	Demoulding and curing in water tank (T = 20 ± 2 °C)	• Three-point bending test to induce cracks with 0.3 mm width (First round). • Optical microscopy. • Ultrasonic measurement.	• Optical microscopy. • Ultrasonic measurement. • Three-point bending test until failure (second round).	• Optical microscopy. • Ultrasonic measurement. • Three-point bending test until failure (third round). • Collection samples for microstructure analysis.
	3			• Optical microscopy. • Ultrasonic measurement. • Second round of three-point bending test until failure. • Collection samples for microstructure analysis.	–
	3			Sorptivity test	–
	3[*]		–	Sorptivity test (uncracked)	–

[*] These three specimens only for the CN mix.

Fig. 4. Three-point flexural test using 2kN INSTRON testing machine.

$$\sigma = \frac{3PL}{2bd^2} \tag{1}$$

$$\varepsilon = \frac{6Dd}{L^2} \tag{2}$$

In the equations, σ is stress in the outer surface at the midpoint (MPa), ε is the strain in the outer surface (mm/mm), P is the load (N), L is the support span (mm), b is the width (mm), d is the depth (mm), and D is the maximum deflection of the prism centre (mm).

The strength recovery after each round was calculated according to Eq. (3) [48]:

$$\text{Efficiency of healing} = \eta\% = \frac{\sigma_2}{\sigma_1} \tag{3}$$

where σ_1 is the maximum stress for the virgin specimen and σ_2 is the maximum stress for the healed specimen.

2.6. Capillary water absorption as a durability indicator

The durability of concrete depends predominantly on the ease with which fluids enter and move through the matrix. Sorptivity is an indicator of concrete's ability to absorb and transmit liquid through it by capillary suction [49]. As stated in RILEM state-of-the-art report [8], measurement of the capillary water absorption for the cracked concrete specimens with and without healing can be used to evaluate the crack healing efficiency. Following the procedure described previously by ASTM C1585 [50] and RILEM report [8], a uni-directional water absorption test was conducted on the healed CN and SHM specimens after 28 days of water curing as indicated in Table 5. As a reference, three uncracked CN specimens were also tested. The specimens were placed in the oven at a temperature of 50 ± 5 °C for 3 days to remove the moisture [50]. Then the area of the cracked surfaces was determined and the adjacent surfaces were covered with sealing adhesive aluminium tape, leaving only the crack face exposed to capillary suction (not more than 10 mm in width) as illustrated schematically in Fig. 6. Only one surface of the specimen was allowed to be in contact with water; the specimens were placed on two rigid non-absorbing supports in a box containing water in such a way that the lower 2 ± 1 mm of the specimens were immersed in water. At regular time intervals for 4 h, the specimens were weighed to determine the weight gain with time. The cumulative absorbed volume i (mm), defined as the change in mass (g) divided by the cross sectional area of the test specimen (mm^2) and the density of water at the recorded temperature (g/mm^3), was plotted against square root of time, $\sqrt{t}$ (min$^{1/2}$). The slope of the obtained line defines the sorptivity index (S) of the specimen during the testing time. For all specimens, this slope is obtained by using least-squares, linear regression analysis of the plot of i versus $\sqrt{t}$.
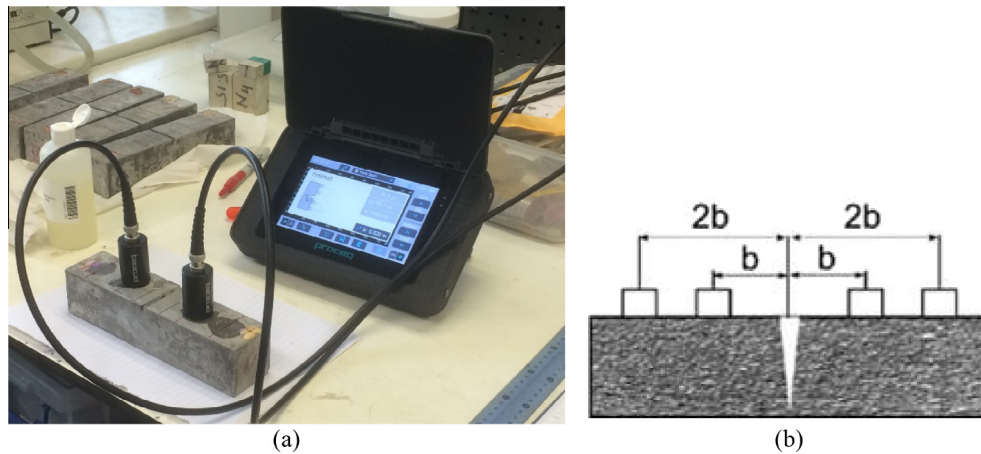
(a)   (b)

Fig. 5. Ultrasonic pulse velocity method for measuring the crack depth of concrete specimens.
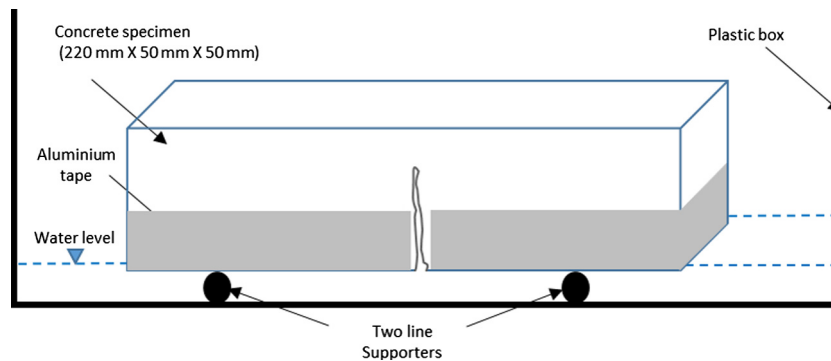

Fig. 6. Schematic diagram of the sorptivity test set-up.

2.7. XRD, FT-IR and SEM analysis

X-ray diffraction analysis (XRD), Fourier transform spectroscopy (FTIR), and scanning electron microscopy (SEM) tests were employed to characterise the developed healing products. As mentioned in the experimental program, the microstructure samples were collected from the area of cracks immediately after the second and third round of three-point bending test. For XRD and FT-IR, powder samples were extracted from the crack planes using DREMEL 3000 rotary tool with steel brush attachment. The collected samples are required to be passing sieve 75 μm. For SEM, small chips of about 5 mm thickness were selected. Thereafter, all samples were immersed in acetone for three days in order to quench any further hydration. Subsequently, they were filtered to remove the acetone followed by vacuum drying in a desiccator. The samples then were put in the oven at 60 °C for at least 24 h and then they were sealed in plastic vials until the time of tests.

XRD was carried out on the Siemens D500 X-ray diffractometer with a CuKα source operating at 40 kV and 40 mA, emitting radiation at a wavelength of 1.5405. The scanning regions were between 2θ values of 10° to 60°, at a rate of 0.05°/step. FTIR spectra of the samples were conducted using Perkin Elmer FTIR Spectrometer Spectrum 100 Optica. Spectra were collected in transmittance mode from 4000 to 600 cm^{-1} at a resolution of 1 cm^{-1}. Scanning electron microscopy (SEM) was conducted using FEI Nova NanoSEM FEG at 15 kV accelerating voltage. Prior to SEM testing, the samples were mounted onto metal stubs using carbon paste and coated with platinum film to ensure good conductivity.

3. Results and discussion

3.1. Evolution of cracks sealing with time (width and depth of cracks)

The sealing of crack surfaces for control and SHM representative samples is shown in Fig. 7. In both samples, crystal depositions can be observed, showing that the control specimens had undergone a certain extent of autogenous healing during immersion in water. Thus, partial filling at the cracks faces can be observed on the control specimens. Crack surfaces at the specimens with sodium silicate impregnated LWA were sealed completely within 28 days.

As the microscopic images can provide an evidence of only the sealing process at the crack surfaces, ultrasonic monitoring was used to evaluate the sealing inside the cracks. Ultrasonic measurements were performed at three different times as indicated in Table 5. The crack depth is measured according to the wave velocity and the propagation path. As the crack plugs with the depositions and fillings, the time of the ultrasonic waves reduces [44]. The average values of the crack depth were plotted against the elapse of time as shown in Fig. 8. The standard deviation is indicated by means of error bars. The SHM specimens exhibited a significant decrease in the crack depth with time. This is evident as the average decrease in the crack depth of SHM specimens was ~80% in 56 days compared to ~21% as an average of the CN specimens. This indicates the influence of sodium silicate in producing more depositions in crack areas to seal them completely.

The mechanism of healing in the vicinity of crack is not entirely evident as the healing could start in different points at the same time as schematically illustrated in Fig. 9. This depends on different parameters such as the number and location of intersected EI-LWA,

(a) CN   (b) SHM
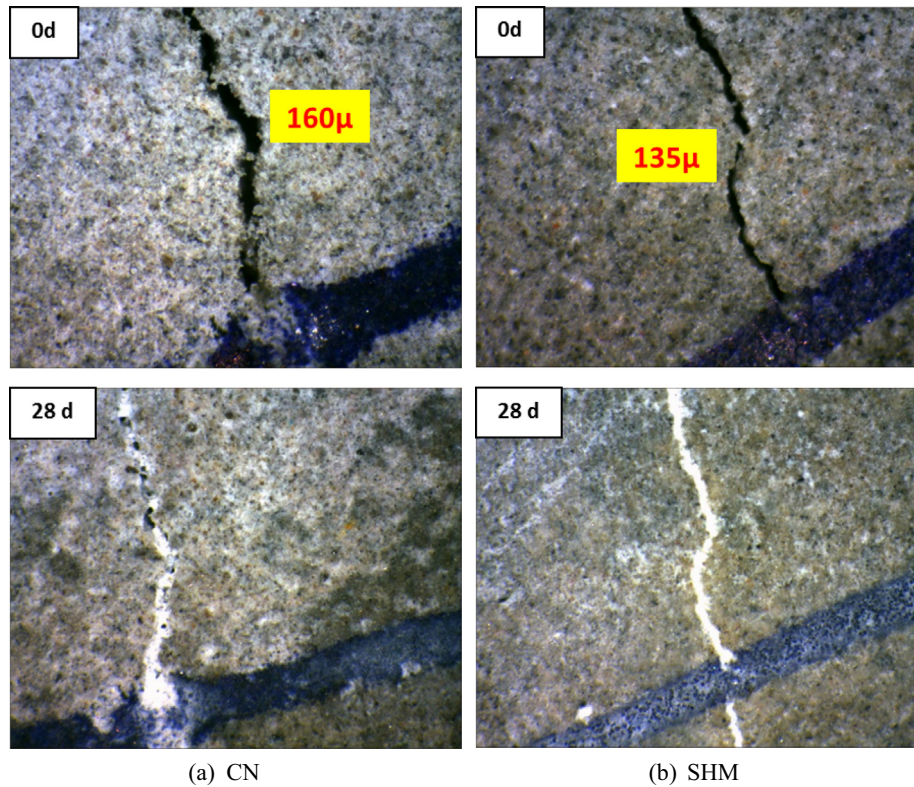
Fig. 7. Representative microscopic images of the crack surfaces immediately after inducing the cracks and after immersed in water for 28 days (a) control sample, and (b) SHM sample.
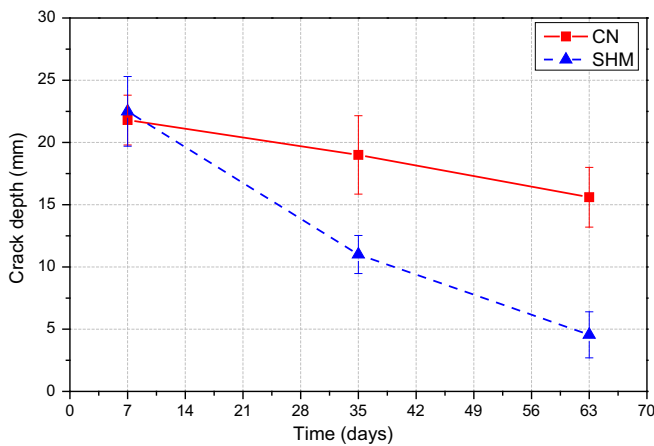
Fig. 8. Crack depth-Ultrasonic Pulse Velocity Method.

the mechanical rupture of the coating, the amount of the healing agent diffused in the crack vicinity, the crack geometry, and the curing conditions. In this study, it is assumed that the healing of the crack initiated mainly from the tip of the crack as dense depositions of the formed healing products aided by ongoing hydration of the cement grains and precipitated concrete fragments as depicted in the area from (b) to (c) in Fig. 9. Simultaneously, the crack surface could be sealed by crystals of calcium carbonates and some healing products, which formed from the adjacent EI-LWA as shown at (a) in Fig. 9. In the CN specimens, the partial healing could be attributed to the ongoing hydration of the cement grains, the precipitation of concrete fragments and potential formation of calcium carbonates. Thus, as illustrated in Fig. 9, the residual depth of crack was assumed to be the distance between

the crack surface (a) and end of dense depositions and healing products at the bottom of the crack vicinity (b).

3.2. Strength recovery

Fig. 10 shows representative flexural stress-strain curves of the two concrete mixes for the three cracking rounds. It can be seen that both specimens behaved similarly at the first round with a slight advantage in the peak value for the control specimen. The CN specimen achieved a maximum stress of 4.55 MPa while the SHM specimen reached 4.40 MPa. This indicates that the impregnation of LWA particles with the sodium silicate solution didn't exhibit adversely effect on the mechanical properties.

In order to assess the strength recovery, six prism specimens from the two mixes were re-cracked once again until failure after 28 days of water curing. The specimens contained the EI-LWA showed 3.55 MPa maximum flexural strength recovery compared with 0.65 MPa for the control specimens (Fig. 10). According to Eq. (3), this could illustrate that the SHM and CN specimen recovered 80% and 14% of their original flexural strength respectively. It is noteworthy here that sodium silicate exhibited 20% and 26% flexural strength recovery when encapsulated in soda glass capsules and polyurethane microcapsules as stated in [45] and [42] respectively. This is an indication of the efficacy of using LWA particles as containers for the self-healing agents in comparison with other techniques. At the third round of cracking, three of the specimens were cracked for the third time until failure after further 28 days of curing in water as presented in the experimental program (Table 5). As shown in Fig. 10, the SHM specimen demonstrated a clear superior of the strength recovery over the control specimen once again: ~1 MPa compared with ~0.4 MPa for the control specimen. In addition, it is obvious that the specimens with the EI-LWA showed much better stiffness recovery than the control
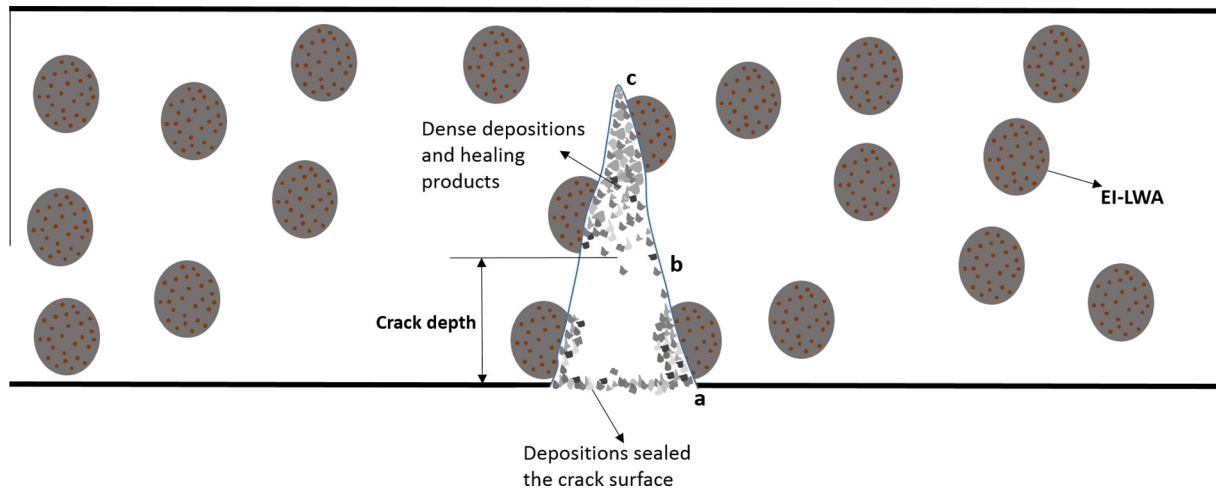
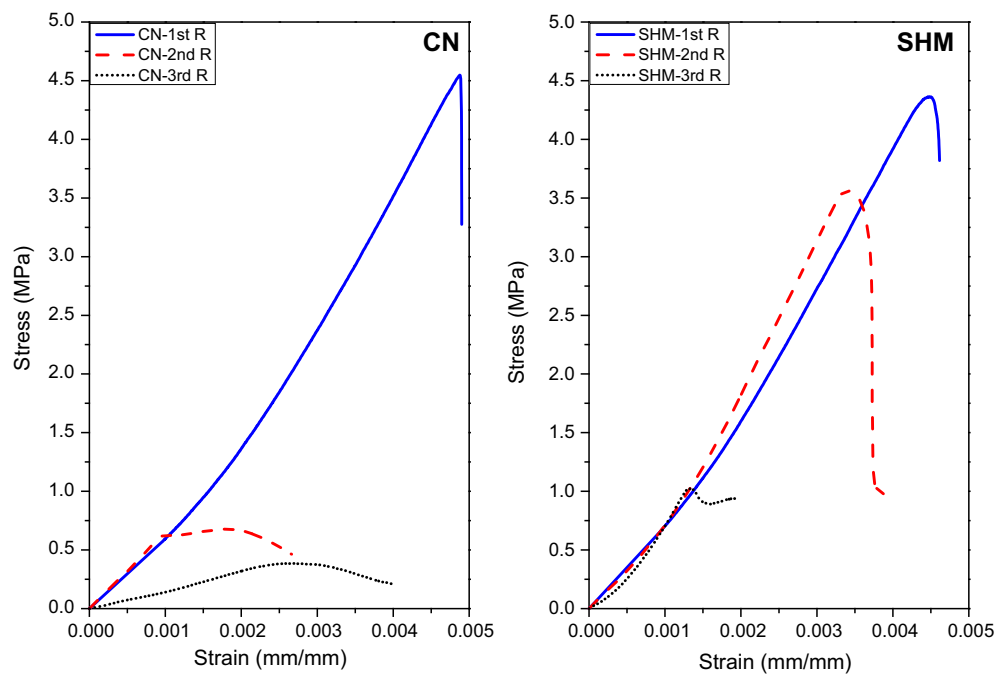**Fig. 9.** Schematic illustration of the healing process in SHM specimen.

Fig. 10. Typical stress-strain curves of the two mixes for the three cracking rounds.

specimens. This can be attributed to the contribution of sodium silicate in forming the healing products in the SHM samples. Once the sodium silicate released from the LWA, it is expected to react with calcium hydroxide, a product of cement hydration, to produce calcium silicate hydrates (C–S–H) gel which allow the recovery of strength [29,42]. The relevant chemical reaction is shown below:

$$Na_2SiO_3 + Ca(OH)_2 \longrightarrow x(CaO \cdot SiO_2) \cdot H_2O + Na_2O \qquad (4)$$
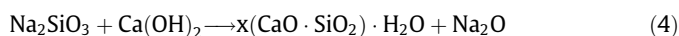
It is well known that the C–S–H as the main reaction product in Portland cement hydration accounts for most of the physical, chemical, and mechanical properties of cements and concretes [51].

3.3. Capillary water absorption and sorptivity index

Plots of the cumulative water absorption against the square root of time are shown in Fig. 11. These plots give the capillary

water absorption through the area of crack after 28 days water curing from inducing the 0.3 mm width cracks in comparison with uncracked CN specimens. It is obvious that the sorptivity values of the healed SHM samples are lower than the healed CN samples. The mean sorptivity coefficient values for the three tested specimens are 0.098 and 0.048 mm/min$^{1/2}$ and the standard deviations are 0.024 and 0.019 for the healed CN and SHM specimens respectively. This implies that the inclusion of EI-LWA led to around 50% reduction of the sorptivity index values in comparison with the values of the control specimens. In addition, the mean sorptivity index of the healed SHM specimens was very similar to the mean sorptivity index of the control uncracked specimens (0.054 mm/min$^{1/2}$). These results indicate that the materials formed in the crack areas of the healed SHM specimens were able to attain complete recovery of the water tightness recovery, which in turn confirms the contribution of sodium silicate in improving the sorption and water tightness properties of the cracked concrete
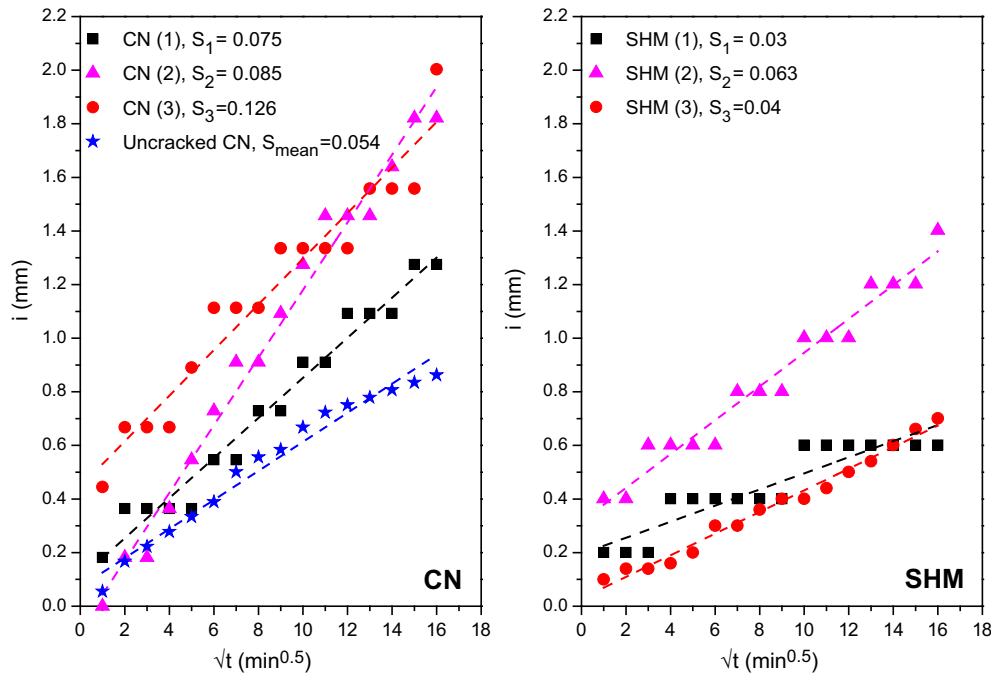
Fig. 11. Cumulative water absorption for the two concrete mixes (a) CN, and (b) SHM.

sections. This is possibly because of the deposition of healing products i.e. C–S–H and sodium silicate crystals reduce the amount of water taken up in the crack by capillary suction.

Both CN and SHM samples showed steadiness of the water absorption rate for different time intervals. However, it is more pronounced in the SHM samples. For instance, SHM (1) samples showed three steady-state intervals within the time of experiment. This could be attributed to the formation of healing products inside the crack area. It is believed that the healing products formed in different points at the same time and in layers upon the availability of the precursor materials in the vicinity of crack as elaborated in Section 3.1. In the control samples, this might be due to the formation of calcium carbonate or in early periods due to the ongoing hydration of the cement grains [10]. In addition to the limited effect of these mechanisms sodium silicate could play a significant role in the crack zone of SHM specimens by producing C–S–H gel due to the reaction with the abundant portlandite in the concrete

matrix. Moreover, it is noteworthy here that the sorptivity test, as standardised, is allocated for one directional flow in uncracked specimens. The water flow in a cracked non-homogenous section is very complicated as water might go through the crack and diffuse laterally; thus sorptivity test has been only used for comparative data in the cracked sections.

3.4. Characterisation of the healing products

Fig. 12 shows the XRD patterns of the healing products collected form the crack areas following the second and third round of cracking. It can be seen that the $Ca(OH)_2$ peaks at $2\theta = 18°$ and at $2\theta = 34.1°$ disappeared completely at the two SHM patterns. In contrast, CN samples showed distinct peaks for the $Ca(OH)_2$. Also, the intensity of the peak at $2\theta = 29.5°$ was stronger in the SHM samples compared with the control samples. This peak is assigned to calcite or C–S–H although C–S–H is generally considered to be
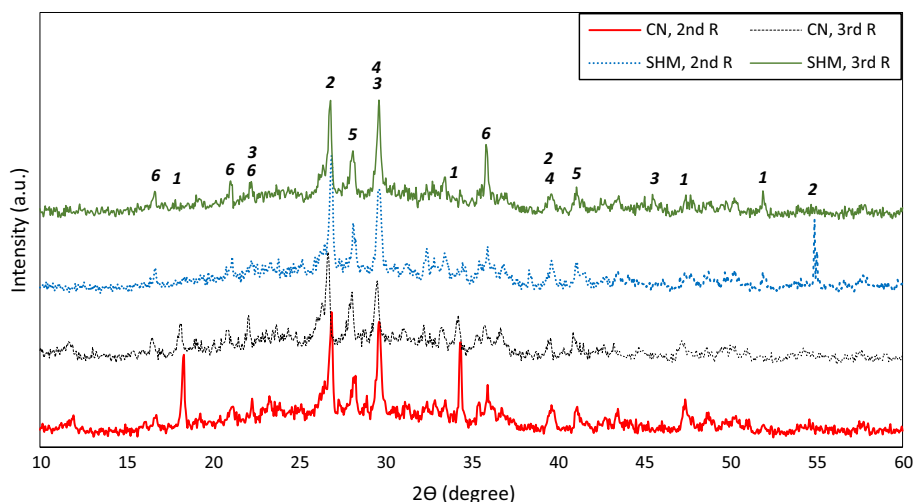

Fig. 12. XRD of the healing products after 2nd round and 3rd round of cracking [**1**: $Ca(OH)_2$; **2**: SiO_2; **3**: $CaCO_3$; **4**: C–S–H; **5**: C_3S/C_2S; **6**: $Ca_6Al_2(SO_4)_3 (OH)_{12}\cdot 26 H_2O$].

poorly crystalline. This confirms the hypothesis that the sodium silicate diffused at the crack planes and reacted with the existent calcium hydroxide to produce more C–S–H gel. SiO_2, C_3S/C_2S and ettringite peaks were detected in all specimens with no significant difference.

Fig. 13 shows the FT-IR spectra of healing products in the cracks of the CN and SHM samples following the second round of cracking. A horizontal axis is shown as wave number (cm^{-1}). The vertical axis (transmittance %) does not indicate any quantitative measurement as the quantities of the sample taken from each mix used in FT-IR test were not equal. The two spectra showed very similar bands as the expected hydration products should be similar. The figure indicates major bands at approximately (1400–1500), (960–1020), and (870–890) cm^{-1}. The bands at 1450 and 860 cm^{-1} suggest the presence of CO_3^{-2}, which can be attributed to the presence of calcite as detected by XRD results. The Si–O band at ~970 cm^{-1} confirms the existence of C–S–H in both samples. However, it is obvious that this Si–O asymmetric stretching band shifted progressively towards greater wavenumber from 966 cm^{-1} for the CN samples to 1017 cm^{-1} for SHM samples. As explained in [52–54], this is an indication of a higher SiO_2 content (silica-rich gel) and more polymerisation in the SHM
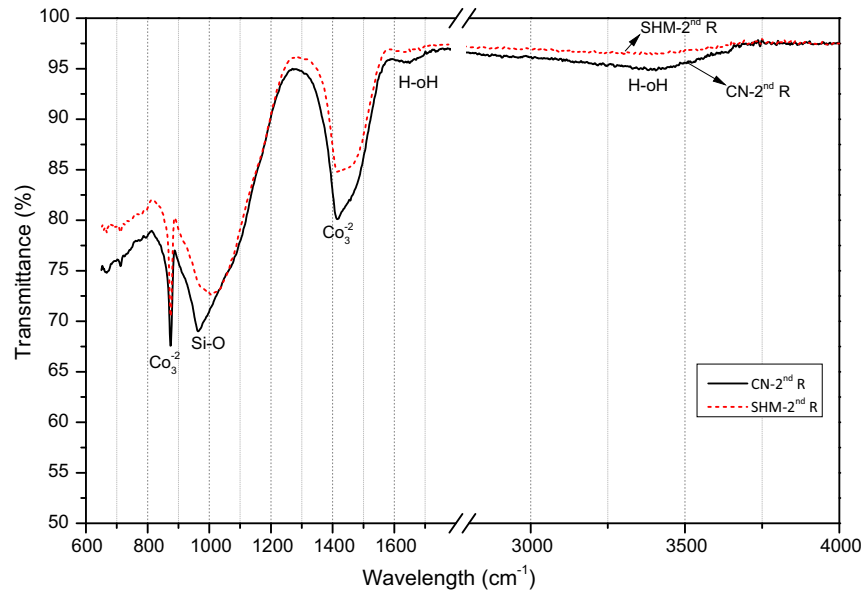

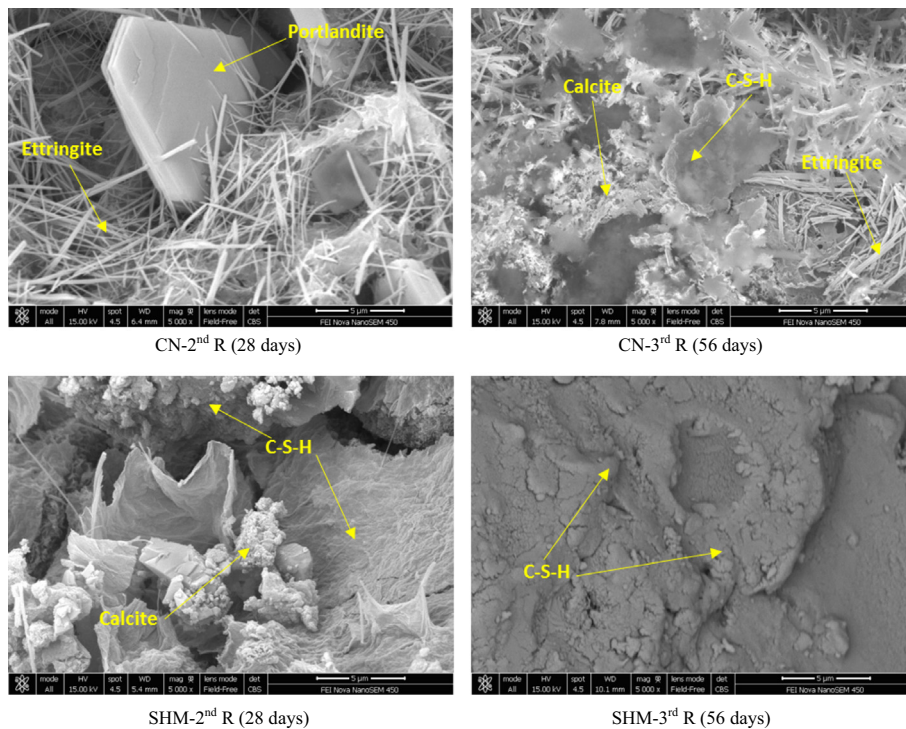Fig. 13. FTIR spectra for the healing product following the 2nd round of cracking.

Fig. 14. BSEM images of healing products at crack surfaces.

samples. This rich silicate gel demonstrates the contribution of the sodium silicate in forming the C–S–H. As the shift in the Si–O band associated with broadening centred at ∼970 cm^{-1}, this could lead to another explanation, which indicates the presence of a two component peak for the SHM specimen between 970 cm^{-1} and 1017 cm^{-1}. These two peaks could be attributed to a blend of CSH (as found in a typical concrete mix) and a silica-rich gel [52]. This is a strong verification of sodium silicate diffusion from LWA particles into the crack area and its contribution in forming the healing products.

SEM images were taken for the healing products at the crack areas as shown in Fig. 14. It can be seen that after 28 days curing in water, the CN specimens developed mainly discrete crystals of ettringite and calcium hydroxide with loose network (Fig. 14a). This contrasts with the SHM samples which developed continuous texture of C–S–H gel with few scattered spots of Calcite (Fig. 14b). These results are in agreement with those obtained by the XRD measurements as the control samples showed stronger peaks of portlandite and ettringite.

Additional 28 days of water curing for specimens after the second round of cracking allowed for further hydration of the existent materials in the area of cracks. In control samples, the content of ettringite and portlandite reduced as some spots of C–S–H gel were appeared (Fig. 14c). However, the SHM sample showed continuous and cohesive texture of C–S–H forming all the highlighted area in Fig. 14d. These observations indicate the contribution of sodium silicate in the SHM samples to produce more C–S–H gel than in the control samples at both ages i.e. 28 and 56 days. This is consistent with the XRD and FTIR observations.

4. Conclusions

In this paper, the impregnation of lightweight aggregates by a liquid self-healing mineral and then their encapsulation in a polymer-based coating layer was suggested as a method for improvement the self-healing performance of concrete composites. The feasibility and efficiency of this method were investigated with reference to strength recovery, water tightness, and crack closure and verified by microstructure analysis for the healing products. Sodium silicate was used as a self-healing agent which has been already employed in a few prior studies.

The SHM specimens showed an effective and remarkable performance in comparison with control specimens in both crack sealing and strength regain parameters. This was achieved without forfeiting the expected mechanical properties of the concrete specimens. For instance, the impregnation of the LWA particles with sodium silicate led to improve strength regain by more than five times and reduce the capillary water absorption to nearly a half. This indicates very promising results compared with many of the other previously suggested techniques.

XRD, FT-IR and SEM techniques are very useful to provide information on the chemical compositions of the healing materials, which support the previous results about the contribution of sodium silicate in producing more calcium silicate hydrate (C–S–H) gel to heal the cracks.

In light of the obtained results, the future work will be focused on employing other minerals as potential self-healing agents and testing other types of lightweight particles to host them. Further investigations about the healing mechanism will be also carried out.

Acknowledgments

Additional data related to this publication is available at the University of Cambridge's institutional data repository: https://www.repository.cam.ac.uk/handle/1810/256105.

References

[1] M. Kessler, N. Sottos, S. White, Self-healing structural composite materials, Compos. Part A Appl. Sci. Manuf. 34 (8) (Aug. 2003) 743–753.
[2] The Strategic Development Council (SDC), Vision 2020. A vision for the concrete repair, protection and strengthening industry, 2004.
[3] V.C. Li, E. Herbert, Robust self-healing concrete for sustainable infrastructure, J. Adv. Concr. Technol. 10 (6) (2012) 207–218.
[4] K. Van Tittelboom, N. De Belie, Self-healing in cementitious materials – a review, Materials (Basel) 6 (6) (May 2013) 2182–2217.
[5] DTI, Construction statistics annual report, London TSO, 2006.
[6] J. Deja, A. Uliasz-Bochenczyk, E. Mokrzycki, CO$_2$ emissions from Polish cement industry, Int. J. Greenhouse Gas Control 4 (4) (2010) 583–588.
[7] U.S. Geological Survey, Mineral commodity summaries: Cement, 2014.
[8] M.R. de Rooij, E. Schlangen, Self-healing phenomena in cement-based materials. State-of-the-Art Report of RILEM Technical Committee 221-SHC, 2011.
[9] H. Huang, G. Ye, C. Qian, E. Schlangen, Self-healing in cementitious materials: materials, methods and service conditions, Mater. Des. 92 (2016) 499–511.
[10] C. Edvardsen, Water permeability and autogenous healing of cracks in concrete, ACI Mater. J. 96 (4) (1999) 448–454.
[11] M. Wu, B. Johannesson, M. Geiker, A review: self-healing in cementitious materials and engineered cementitious composite as a self-healing material, Constr. Build. Mater. 28 (1) (Mar. 2012) 571–583.
[12] N. ter Heide, E. Schlangen, Self-healing of early age cracks in concrete, First International Conference on Self Healing Materials, April 2007, pp. 1–12.
[13] H.-W. Reinhardt, M. Jooss, Permeability and self-healing of cracked concrete as a function of temperature and crack width, Cem. Concr. Res. 33 (7) (Jul. 2003) 981–985.
[14] H. Mihashi, T. Nishiwaki, Development of engineered self-healing and self-repairing concrete-state-of-the-art report, J. Adv. Concr. Technol. 10 (5) (2012) 170–184.
[15] V.C. Li, Y.M. Lim, Y.-W. Chan, Feasibility study of a passive smart self-healing cementitious composite, Compos. Part B Eng. 29 (6) (Nov. 1998) 819–827.
[16] M. Şahmaran, V.C. Li, Durability properties of micro-cracked ECC containing high volumes fly ash, Cem. Concr. Res. 39 (11) (Nov. 2009) 1033–1043.
[17] Y. Yang, E.-H. Yang, V.C. Li, Autogenous healing of engineered cementitious composites at early age, Cem. Concr. Res. 41 (2) (Feb. 2011) 176–183.
[18] T. Nishiwaki, M. Koda, M. Yamada, H. Mihashi, T. Kikuta, Experimental study on self-healing capability of FRCC using different types of synthetic fibers, J. Adv. Technol. 10 (6) (2012) 195–206.
[19] D. Snoeck, S. Steuperaert, K. Van Tittelboom, P. Dubruel, N. De Belie, Visualization of water penetration in cementitious materials with superabsorbent polymers by means of neutron radiography, Cem. Concr. Res. 42 (8) (Aug. 2012) 1113–1121.
[20] H. Lee, Potential of superabsorbent polymer for self-sealing cracks in concrete, Adv. Appl. Ceram. 109 (5) (2010).
[21] N. Ter Heide, Crack Healing in Hydrating Concrete, Delft Univ. Technol., Delft, 2005.
[22] E. Gruyaert, K. Van Tittelboom, H. Rahier, N. De Belie, Crack repair by activation of the pozzolanic or slag reaction, 2nd International Conference on Microstructural-related Durability of Cementitious Composites, 2012, pp. 1–8.
[23] P. Termkhajornkit, T. Nawa, Y. Yamashiro, T. Saito, Self-healing ability of fly ash–cement systems, Cem. Concr. Compos. 31 (3) (Mar. 2009) 195–203.
[24] D. Jaroenratanapirom, R. Sahamitmongkol, Effects of different mineral additives and cracking ages on self-healing performance of mortar, Proceedings of the 6th Annual Concrete Conference, Phetchaburi, Thailand, 2010, pp. 551–556.
[25] Y. Zhao, J. Fickert, K. Landfester, D. Crespy, Encapsulation of self-healing agents in polymer nanocapsules, Small 8 (19) (Oct. 2012) 2954–2958.
[26] T.D.P. Thao, T.J.S. Johnson, Q.S. Tong, P.S. Dai, 'Implementation of self-healing in concrete – Proof of concept', IES J. Part A Civ. Struct. Eng. 2 (2) (2009) 116–125.
[27] H. Mihashi, Y. Kaneko, T. Nishiwaki, K. Otsuka, Fundamental study on development of intelligent concrete characterized by self-healing capability for strength, Trans. Japan Concr. Inst. 22 (2001) 441–450.
[28] C. Dry, Three-part methylmethacrylate adhesive system as an internal delivery system for smart responsive concrete, Smart Mater. Struct. 5 (3) (Jun. 1996) 297–300.
[29] H. Huang, G. Ye, C. Leung, K.T. Wan, Application of sodium silicate solution as self-healing agent in cementitious materials, International RILEM Conference on Advances in Construction Materials through Science and Engineering (2011) 530–536.

[30] C.M. Dry, Three designs for the internal release of sealants, adhesives, and waterproofing chemicals into concrete to reduce permeability, Cem. Concr. Res. 30 (12) (2000) 1969–1977.

[31] C.M. Dry, Repair and prevention of damage due to transverse shrinkage cracks in bridge decks, 1999 Symposium on Smart Structures and Materials (1999) 253–256.

[32] C. Joseph, A.D. Jefferson, M.B. Cantoni, Issues relating to the autonomic healing of cementitious materials, Proc. First Int. Conf. Self Heal. Mater., April 2007, pp. 1–8.

[33] K. Van Tittelboom, N. De Belie, W. De Muynck, W. Verstraete, Use of bacteria to repair cracks in concrete, Cem. Concr. Res. 40 (1) (Jan. 2010) 157–166.

[34] V. Wiktor, H.M. Jonkers, Quantification of crack-healing in novel bacteria-based self-healing concrete, Cem. Concr. Compos. 33 (7) (Aug. 2011) 763–770.

[35] J.Y. Wang, D. Snoeck, S. Van Vlierberghe, W. Verstraete, N. De Belie, Application of hydrogel encapsulated carbonate precipitating bacteria for approaching a realistic self-healing in concrete, Constr. Build. Mater. 68 (Oct. 2014) 110–119.

[36] T. Kishi, T.H. Ahn, A. Hosoda, S. Suzuki, H. Takaoka, Self-healing behaviour by cementitious recrystallization of cracked concrete incorporating expansive agent, Proceedings of the First International Conference on Self-Healing Materials, Noordwijk aan zee, the Netherlands, 2007.

[37] L. Ferrara, V. Krelani, M. Carsana, A "fracture testing" based approach to assess crack healing of concrete with and without crystalline admixtures, Constr. Build. Mater. 68 (2014) 535–551.

[38] M. Roig-Flores, S. Moscato, P. Serna, L. Ferrara, Self-healing capability of concrete with crystalline admixtures in different environments, Constr. Build. Mater. 86 (2015) 1–11.

[39] K. Sisomphon, O. Copuroglu, E.A.B. Koenders, Surface crack self-healing behaviour of mortars with expansive additives, 3rd International Conference on Self-healing Materials, Bath, UK, 2011, pp. 44–45.

[40] A. Hosoda, T. Kishi, H. Arita, Y. Takakuwa, Self healing of crack and water permeability of expansive concrete, 1st International Conference on Self-Healing Materials. Noordwijk, Holland, 2007.

[41] R. Alghamri, A. Al-Tabbaa, Self-healing of cementitious composites via coated magnesium oxide/silica fume based pellets, 27th Biennial Concrete Institute of Australia's National Conference in Conjunction with the 69th RILEM Week Conference, 2015.

[42] M.M. Pelletier, R. Brown, A. Shukla, A. Bose, Self-Healing Concrete with a Microencapsulated Healing Agent, Univ. Rhode Island, Kingston, USA, 2011.

[43] J. Gilford III, M.M. Hassan, T. Rupnow, M. Barbato, A. Okeil, S. Asadi, Dicyclopentadiene and sodium silicate microencapsulation for self-healing of concrete, J. Mater. Civ. Eng. 26 (5) (2014) 886–896.

[44] E. Mostavi, S. Asadi, M.M. Hassan, M. Alansari, Evaluation of self-healing mechanisms in concrete with double-walled sodium silicate microcapsules, J. Mater. Civ. Eng. (2015). p. 04015035.

[45] A. Kanellopoulos, T.S. Qureshi, A. Al-Tabbaa, Glass encapsulated minerals for self-healing in cement based composites, Constr. Build. Mater. 98 (2015) 780–791.

[46] K. Sisomphon, O. Copuroglu, A. Fraaij, Application of encapsulated lightweight aggregate impregnated with sodium monofluorophosphate as a self-healing agent in blast furnace slag mortar, Heron 56 (1/2) (2011) 13–32.

[47] Lytag, Technical Manual – Section 3 Mix Designs for Lytag Concrete, 2006.

[48] B. Aïssa, D. Therriault, E. Haddad, W. Jamroz, Self-healing materials systems: overview of major approaches and recent developed technologies, Adv. Mater. Sci. Eng. 2012 (2012) 1–17.

[49] B.B. Sabir, S. Wild, M. O'Farrell, A water sorptivity test for mortar and concrete, Mater. Struct. 31 (8) (1998) 568–574.

[50] M. Şahmaran, S.B. Keskin, G. Ozerkan, I.O. Yaman, Self-healing of mechanically-loaded self consolidating concretes with high volumes of fly ash, Cem. Concr. Compos. 30 (10) (Nov. 2008) 872–879.

[51] H.F.W. Taylor, Cement Chemistry, Thomas Telford, 1997.

[52] S.Y. Hong, F.P. Glasser, Alkali sorption by C-S-H and C-A-S-H gels: part II. Role of alumina, Cem. Concr. Res. 32 (7) (2002) 1101–1111.

[53] C.K. Yip, G.C. Lukey, J.S.J. van Deventer, The coexistence of geopolymeric gel and calcium silicate hydrate at the early stage of alkaline activation, Cem. Concr. Res. 35 (9) (2005) 1688–1697.

[54] I. García-Lodeiro, A. Fernández-Jiménez, M.T. Blanco, A. Palomo, FTIR study of the sol-gel synthesis of cementitious gels: C-S-H and N-A-S-H, J. Sol-Gel Sci. Technol. 45 (1) (2008) 63–72.